



Available online at www.sciencedirect.com

ScienceDirect

journal homepage: www.journals.elsevier.com/oceanologia/



ORIGINAL RESEARCH ARTICLE

Erosion and deposition processes from field experiments of hydrodynamics in the coastal mangrove area of Can Gio, Vietnam

Hoa Tien Le Nguyen^{*}, Hong Phuoc Vo Luong

Department of Oceanology, Meteorology and Hydrology, University of Science, Vietnam National University, Ho Chi Minh City, Vietnam

Received 16 August 2018; accepted 23 November 2018
Available online 1 December 2018

KEYWORDS

Hydrodynamics;
Suspended sediment concentrations (SSCs);
Erosion;
Mangrove forests;
Can Gio Mangrove Biosphere Reserve

Summary Studying hydrodynamic processes is necessary for understanding the sediment erosion–deposition mechanism in mangrove areas. The hydrodynamic effects within the mangrove area of the Dong Tranh Estuary in the Can Gio Mangrove Biosphere Reserve in Ho Chi Minh City (HCMC), Vietnam are very complicated and are caused by the mixed impacts of waves, tides, currents and suspended sediment concentrations (SSCs). In this study, the measurements of hydrodynamics such as waves, currents and SSCs were conducted in the dry (Feb. 2012) and wet (Jun. 2014) seasons. Three stations were set up within the estuary, mud-flat and mangrove forest. The analysed results showed that the hydrodynamics in all three stations were strongly influenced during the first dry monsoon season and the next wet one. The waves were the main factor during the dry season and contributed more SSC turbulence in the mud-flat, potentially causing erosion at the study site. Meanwhile, the current velocities in both the estuary and mud-flat sites were major factors during the wet season. In the mangrove forest, the SSC during the dry season changed due to the tidal cycle. Additionally, two measurements for the change in the topographies and shorelines were conducted from 2014 to 2017. The results show that the study site has been eroding rapidly ($0.61 \text{ m month}^{-1}$). Although this study shows a soil retention role for the mangrove forests, the wave energy dissipation occurs mainly within the mud-flat due to the bottom topography. The study site is proven to be eroding.

© 2018 Institute of Oceanology of the Polish Academy of Sciences. Production and hosting by Elsevier Sp. z o.o. This is an open access article under the CC BY-NC-ND license (<http://creativecommons.org/licenses/by-nc-nd/4.0/>).

^{*} Corresponding author at: Vietnam National University, 227 Nguyen Van Cu Street, Ward 4, District 5, Ho Chi Minh City, Vietnam. Tel.: +84 916716013. Fax: +84 28 3835 8463.

E-mail addresses: lnhtien@hcmus.edu.vn (H.T. Le Nguyen), vlhphuoc@hcmus.edu.vn (H.P. Vo Luong).

Peer review under the responsibility of Institute of Oceanology of the Polish Academy of Sciences.



Production and hosting by Elsevier

<https://doi.org/10.1016/j.oceano.2018.11.004>

0078-3234/© 2018 Institute of Oceanology of the Polish Academy of Sciences. Production and hosting by Elsevier Sp. z o.o. This is an open access article under the CC BY-NC-ND license (<http://creativecommons.org/licenses/by-nc-nd/4.0/>).

1. Introduction

Mangrove forests occupy the entire intertidal zone along the tropical and subtropical coastlines, which play an important role in reducing coastal erosion. Mangroves often protect coastlines due to their ability to dissipate wave energy (Cao et al., 2016; Horstman et al., 2014; Massel et al., 1999; Parvathy and Bhaskaran, 2017; Vo-Luong and Massel, 2006). Many species of mangroves also have extensive cable root systems that assist in binding the sediment particles. In this way, mangrove-covered shorelines are less likely to erode or will erode more slowly than unvegetated shorelines during periods of high wave energy (Saenger, 2002). In addition, salt marshes or mangrove forest have value for coastal hazard mitigation and climate change adaptation with three specific ecosystem services: wave attenuation, shoreline stabilisation, and floodwater attenuation (Shepard et al., 2011).

There are various studies about the hydrodynamic processes in mangrove forests. Wolanski (1995) presented the principles of the processes that directly impact the sediment transport in mangrove forests, and, later, Furukawa and Wolanski (1996) described the structure, distribution and settling velocity of the agglutinate sediment. Bryce et al. (2003) studied the hydrodynamic and geomorphological controls on suspended sediment transport in mangrove creek systems with a case study in Cocoa Creek, Townsville, Australia. Capo et al. (2006) measured and analysed the surface sediment as well as the suspended sediment concentrations (SSCs) in the mangrove forest in Konkoure Estuary, Guine. Recently, from practical surveys and the application of two numerical models, FVCOM and ESSed, Li et al. (2014) showed the effects of the mangrove forests and intertidal areas on the dynamics of suspended sediment in the Darwin seaport, Australia.

In Vietnam, which has 270,000 hectares of mangrove forests (FAO, 2015), many hydrodynamic studies have been done. Mazda et al. (1997, 2006) showed that the mangrove forests can attenuate the wave energy in the Tong King Delta. Van Santen et al. (2007) studied a mangrove system in the Ba Lat Estuary of the Red River in the dry season (Feb./Mar. 2000) and in the wet season (Jul./Aug. 2000). The study demonstrated that the bare mud bank of an estuary is highly dynamic until the mangroves cover it. Although the sediment delivery to the vegetated zones is low, the protective effect of the vegetation against erosion by the waves and currents is high. Bao (2011) studied at two coastal mangrove forest areas in Vietnam, including the Red River Delta and Can Gio mangrove forests, and showed that the wave height decays exponentially with the distance from the mangrove front. Norris et al. (2017) examined the role of pneumatophores as a spatial control on the dissipation of the turbulent kinetic energy in the southern edge of Cu Lao Dung in the Mekong Delta. The turbulent dissipation reaches its maximum at the forest fringe, where pneumatophore densities are the highest. The dissipation depends on the tides, wave heights and water depths. High turbulent energy at the forest fringe may suspend fine sediments that can be redistributed elsewhere in the forest.

Can Gio was designated as the first Mangrove Biosphere Reserve in Vietnam under the Man and the Biosphere Programme of UNESCO in 2000 (Vo Quoc and Kuenzer, 2012). Can Gio is an ideal scientific research area. Mazda et al. (2002) determined the erosion mechanism of the coast of Long Hoa

village. The first necessary condition is that the strong tidal flows move the bottom sediments along the coast of Long Hoa alongside the river mouths. The second condition is that the changes in the mangrove vegetation density due to human intervention have prevented the amplitude of the tidal flows from becoming steady. Therefore, the erosion is due to the tidal forces and not due to the wave action. Vo-Luong and Massel (2006, 2008) measured and studied the Nang Hai Creek at Dong Tranh Estuary for two years (2004 and 2005), mainly during the dry season. The results prove that the effect of the wave breaking plays an important role on the wave attenuation in a sparse forest. Waves are one of the primary factors that influence the sediment transport and cause coastal erosion, even though the wave fields are rather weak. However, the results are estimated and analysed only during the North East monsoon. Vo Luong (2012) used a “tracer stick” method and “coloured sample” method to measure the erosion and deposition of the surface sediment in Nang Hai Creek. The results showed that there is a clear occurrence of erosion–deposition processes, and the erosion process is dominant. In addition, the author applied a one-dimensional model to calculate the vertical SSCs. The results showed that SSCs at the bottom are much higher than those at the surface. The results also prove that SSCs depend on the wave intensity and tidal current velocity, thus concluding that the mangrove vegetation can encourage the deposition of sediment and protect the coastland from high waves and storms. Bay et al. (2012) suggested a mathematical model to simulate the sediment transport affected by the tides and winds in which the numerical results showed a trend of sediment accretion-erosion and concurred with the satellite observations. However, it is important to note that the model does not mention the mangrove forests and only simulates the sediment transport on the coastal zone of Can Gio. Vinh and Truong (2012) carried out a field investigation, GIS and numerical modelling (MIKE 21) to determine and analyse the erosion mechanism in the Nga Bay River and found that the actual erosion rate is approximately 10 m year^{-1} . The main factors found were currents, waves and ship-generated waves. However, the authors only studied the erosion mechanism in the riverbanks and river mouth. Recently, Schwarzer et al. (2016) studied the sediment dynamics in a mangrove forest on time-scales from the spring-neap tidal cycles to the seasonal cycles (dry season versus wet season) to investigate the inter-tidal sediments forming the forest soil and the suspended matter dynamics in a creek that floods and discharges in the mangrove forest. The study was conducted in the Khe Nhan Creek, Rach Oc Creek and Nang Hai Creek in the Dong Tranh River.

Those studies showed that the mangrove forests in Can Gio are faced with high risks of erosion, especially in the Dong Tranh River and Nga Bay River Mouth. Hence, it is necessary to increase the research relevant to the dynamic factors for the coastal stabilisation and erosion mechanisms in mangrove forests.

Therefore, the aims of this study are to evaluate and explain the main hydrodynamics impact on erosion and deposition processes in mangrove areas. The measured and observed data of the hydrodynamics in mangrove areas, such as waves, currents, tides and SSCs, have been worked out in the Nang Hai site at Can Gio (HCMC) in the dry season (Feb. 2012) and the wet season (Jun. 2014). Furthermore, the study

measures and analyses the changes in the measured shorelines and topographies at the study site from 2014 to 2017.

2. Data collection

2.1. Study site

The field experiments for this study were done in the mangrove region in the Dong Tranh River (Fig. 1a). This region is a branch of the Saigon-Dong Nai River located in the HCMC, Vietnam (Hong and San, 1993). The study site was located between the Capes Ly Nhon and Long Hoa side of the estuary; therefore, it was less affected by the strong wind-induced waves (Vo-Luong and Massel, 2006). The tidal regime in Can Gio is an irregular semi-diurnal regime with an average tidal

amplitude from 2 m (mean tide) to 4 m (spring tides) (Vo Quoc and Kuenzer, 2012).

The Nang Hai mangrove area was chosen as the study site and equipped with three stations: ST0 in the estuary (Fig. 1c), ST1 in the mud-flat and ST2 in the mangrove forest (Fig. 1b). Station ST1 and ST2 are approximately 2000 m apart from ST0. Station ST1 is approximately 30 m from ST2. The positions of the three stations were:

- Station in the estuary (ST0): 10°22'46.38"N; 106°51'57.12"E,
- Station in the mud-flat (ST1): 10°23'27.18"N; 106°52'48.12"E,
- Station in the mangrove forest (ST2): 10°23'27.43"N; 106°52'49.31"E.

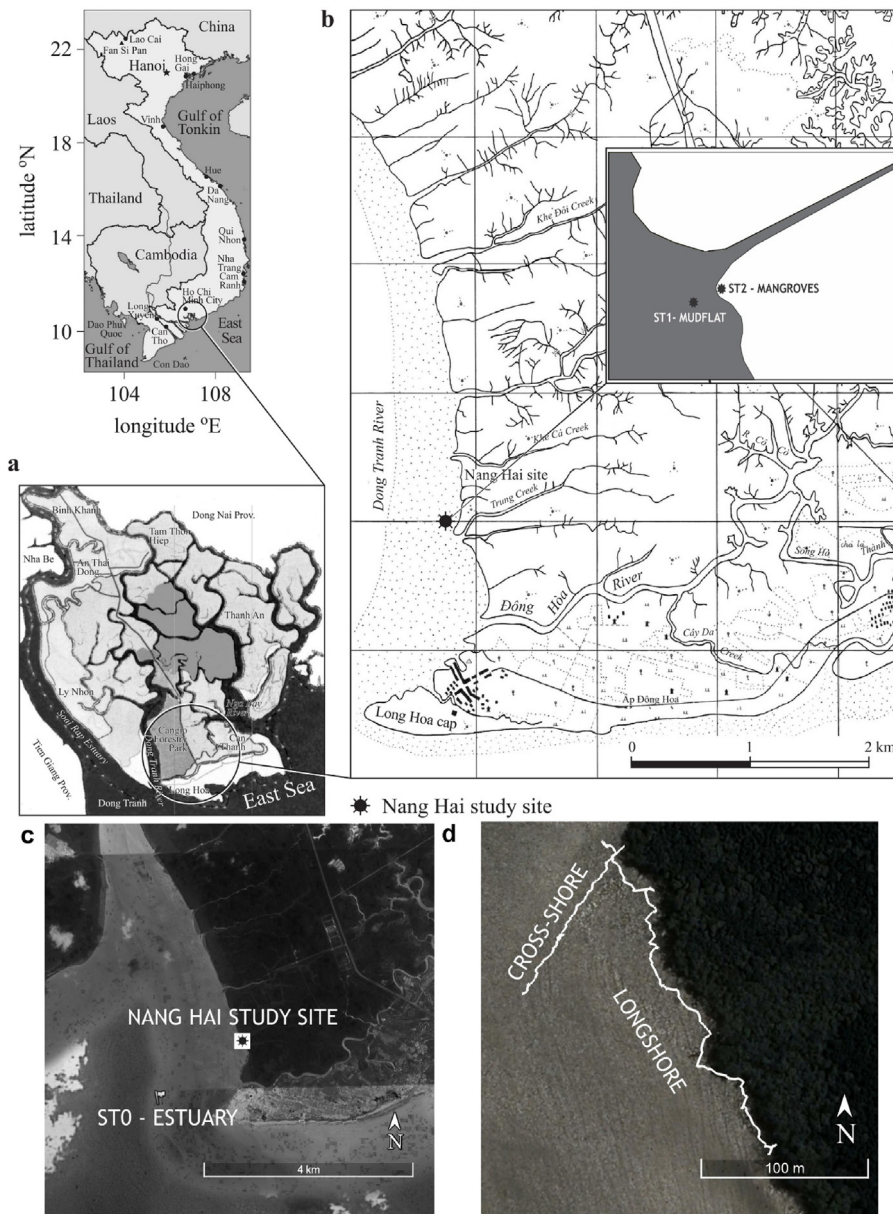


Figure 1 Location of the experimental area: (a) Vietnam and Can Gio Mangrove Biosphere Reserve, HCMC, Vietnam; (b) Nang Hai study site; (c) station ST0 in the estuary and (d) the measured cross-shore profile and measured longshore transect.

Table 1 The physical settings of the instruments at the study site.

Instruments	Measured factors	Physical settings
Valeport MIDAS DWR 27110	Water level	Sampling rate [Hz]: 4
	Current	Interval [mins]: 30
Valeport MIDAS DWR 27111	Turbidity [mV]	No. of samples: 2048
	Wave	
AEM-213D	Current	Interval [mins]: 60 No. of samples: 4800
INFINITY-Turbi ATU75W2	Turbidity [FTU]	Interval [mins]: 60 No. of samples: 4800
INFINITY-WH	Wave	Interval [mins]: 30 No. of samples: 4800

The field experiments were conducted during the dry season (Feb. 2012) and wet season (Jun. 2014), and every field campaign completed lasted for seven days. The primary measured factors were the water level depths, current velocities, wave heights and SSCs (from turbidity measurements). Additionally, the changes in the shorelines and topographies were measured from 2014 to 2017 (Fig. 1d).

2.2. Methods

2.2.1. Hydrodynamics

The measurements of the hydrodynamic factors were obtained by using various types of instruments: Valeport MIDAS DWR, AEM-213D, AEM-USB, INFINITY-Turbi ATU75W2 and INFINITY-WH (Table 1). The Valeport MIDAS DWR was fitted with sensors to measure the water level depths, current velocities, wave heights and SSCs (from turbidity measurements) (Fig. 2a). The instruments AEM-213D, INFINITY-

Turbi ATU75W2 and INFINITY-WH had sensors levelled at 5 cm above the bottom bed (Fig. 2b). Table 2 shows the positions of the instruments at the study site in the dry and wet seasons.

2.2.2. Suspended sediment concentrations

To measure SSCs, the instruments required calibration. In the field experiments, the units of concentration in the instruments are mV (for Valeport MIDAS DWR) or FTU (for INFINITY-Turbi ATU75W2) (Fig. 2a and b). To convert the FTU/mV values into real concentrations, the water samples were required for calibration. The water samples were taken every 30–60 min within 24 h at all three stations. Then, the water samples were analysed in the laboratory (Fig. 2c).

2.2.3. Topography and shoreline changes

To analyse the changes of the topography and shoreline, data was collected in two ways (Fig. 1d):

- *Longshore changes*: the shoreline is considered to be the boundary between the mangroves and the mud-flat. The length of the measured boundary was 200 m (Fig. 1d). By using the GPS map 76CSx, data was collected along the mangrove boundary from 2014 to 2017. In total, four analyses were recorded on 20th Jan. 2014, 4th Feb. 2015, 17th Dec. 2016 and 25th May 2017. The data was processed by the DSAS tool (Digital Shoreline Analysis System) in ArcGIS 10.3.
- *Cross-shore changes*: the measured profile extended from the mangrove forests to the mud-flat and passed through the boundary. The measured length of the profile was approximately 120–140 m from the mangrove to the mud-flat in intervals of 1–2 m. Three referenced points were set up at the boundary, the mud-flat and the mangrove. The referenced point at the boundary was called the “zero point”. The distance from the zero point to the mangrove is approximately 20–40 m. The distance from the zero point to the mud-flat is approximately 100 m. The SOKKIA level instrument was used eight times to measure on the dates: 20th Jan. 2014, 25th Jun. 2014, 26th Nov. 2014, 4th Feb. 2015, 19th Oct.



(a) Valeport at station ST1



(b) AEM, INFINITI Turbi and INFINITI WH at station ST2



(c) Water sample filtration in the laboratory

Figure 2 Measuring at the study site (a, b) and the water sample filtration in the laboratory (c).

Table 2 Observed time and positions of the instruments.

Stations	The dry season (Feb. 6th–13th, 2012)	The wet season (Jun. 20th–26th, 2014)
ST0	Valeport MIDAS DWR 27110 (Feb. 6th–9th, 2012)	Valeport MIDAS DWR 27111
ST1	Valeport MIDAS DWR 27111	- Valeport MIDAS DWR 27110 - AEM-213D
ST2	Valeport MIDAS DWR 27110 (Feb. 9th–13th, 2012)	- AEM-USB - INFINITY-Turbi ATU75W2 - INFINITY-WH

2015, 12th Jan. 2016, 18th Dec. 2016 and 25th May 2017. There were seven phases as follows:

- The first phase (20th Jan. 2014–25th Jun. 2014): dominant dry season,
- The second phase (25th Jun. 2014–26th Nov. 2014): dominant wet season,
- The third phase (26th Nov. 2014–4th Feb. 2015): dry season,
- The fourth phase (4th Feb. 2015–19th Oct. 2015): dominant wet season,
- The fifth phase (19th Oct. 2015–12th Jan. 2016): dominant dry season,
- The sixth phase (12th Jan. 2016–18th Dec. 2016): both seasons,
- The seventh phase (Dec. 2016–25th May 2017): dominant dry season.

2.3. Calibration results

From the data analysed in the laboratory and the field experiments, there were a total of five results for the correlation between the analysed SSCs and the recorded output from the instrument sensors (D&A Ins Co., 2004). Fig. 3 is an example for the calibration result at station ST0 in the estuary. All results show that the value of R -squared is between 63% and 91%. The calibration results are highly reliable. The regression equations of every station are as follows:

In the dry season (Feb. 2012):

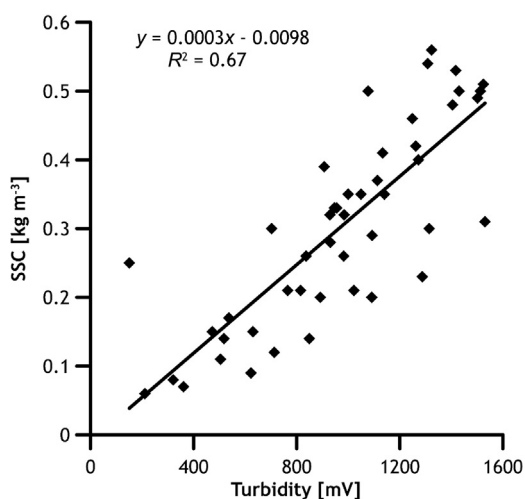


Figure 3 An example of the calibration results of Valeport MIDAS DWR at station ST0 in the estuary.

- ST0 and ST2: $y = 0.0074x + 0.0069$; $R^2 = 0.90$
- ST1: $y = 0.0003x + 0.0174$; $R^2 = 0.91$

In the wet season (Jun. 2014):

- ST0: $y = 0.0003x - 0.0098$; $R^2 = 0.67$
- ST1: $y = 0.0025x + 0.0509$; $R^2 = 0.73$
- ST2: $y = 0.0001x$; $R^2 = 0.63$

where y : SSC – [kg m^{-3}], x : record output – [mV] or [FTU].

3. Results

3.1. In the estuary

In the estuary (ST0), the tidal ranges during both seasons were found to be approximately the same (3.30 m in the dry season (Fig. 4a) and 3.20 m in the wet season (Fig. 4d)), while the current velocity data showed minor changes and a small variance between the seasons (0.19 m s^{-1} in the dry season (Fig. 4b) and 0.15 m s^{-1} in the wet season (Fig. 4e)). However, the significant wave heights in the dry season (Fig. 4c) were much higher than the ones in the wet season (Fig. 4f), as they were recorded to reach up to 0.55 m in the dry season but only approximately 0.24 m in the wet season. Consequently, the average SSCs in the dry season (0.15 kg m^{-3} – Fig. 4a) were higher than in the wet season (0.10 kg m^{-3} – Fig. 4d).

The results show that during the dry season, the SSCs were affected by the water level fluctuations, current velocities and significant wave heights (Fig. 4a–c). On the two first tidal days, the waves were weak (Fig. 4c) but the current velocities (Fig. 4b) and the SSCs (Fig. 4a) were high. Especially during the third tidal day, the SSC reached its highest values because the significant wave heights and the current velocities values reached their recorded peaks. Therefore, the waves had a strong impact on the variability of SSCs at station ST0 during the dry season. In contrast, during the wet season, the relationship between SSCs and waves was weaker than the relationship between SSCs and current velocities. With the increase of the current velocities, the SSCs also increased; hence, in the wet season, SSCs are mainly controlled by the currents. In general, any changes in the hydrodynamics will have a direct influence on SSCs in both the dry and wet seasons.

3.2. In the mud-flat

In the mud-flat (ST1), the results show that the water levels in the dry season (Fig. 5a) are higher than the ones in the wet season (Fig. 5d). The maximum water level was 2.26 m in the

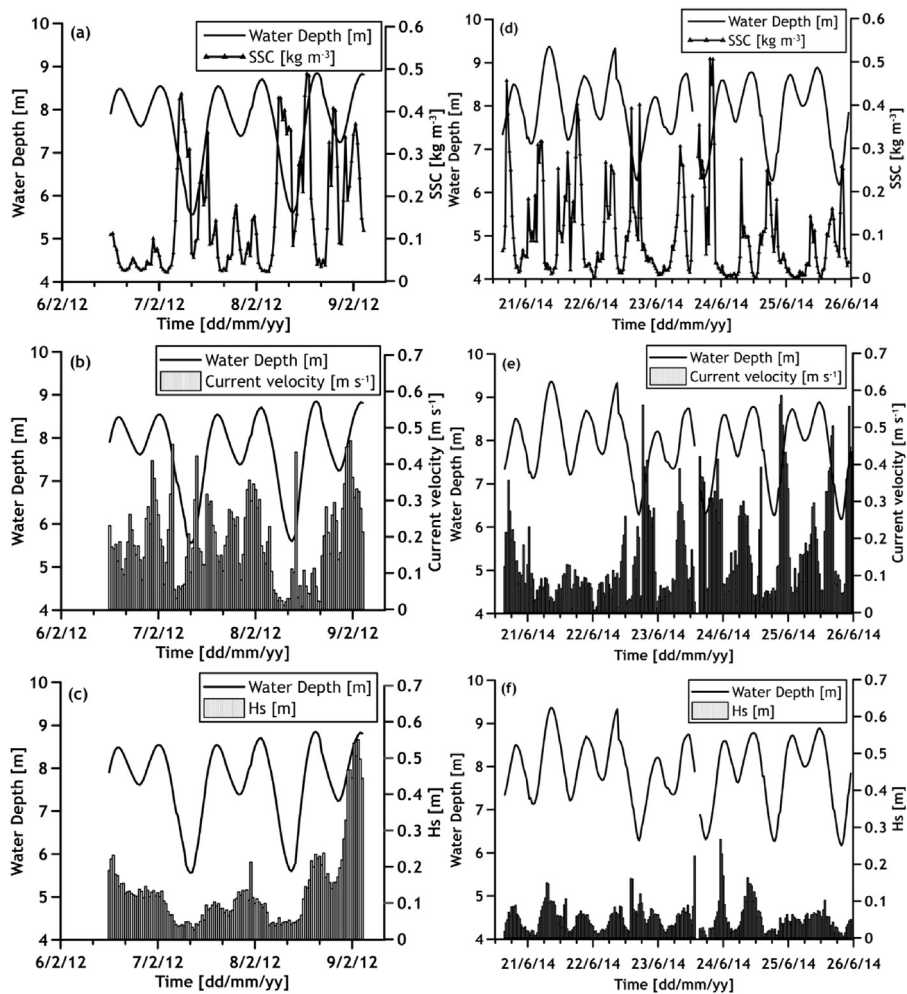


Figure 4 Water depths, SSCs, current velocities, and significant wave heights (Hs) in the estuary (STO) in the dry season (a–c) and in the wet season (d–f).

dry season and 1.68 m in the wet season. However, the current velocities in both seasons were low, recording only 0.12 m s^{-1} as its maximum. The results show that the flood current velocities were higher than the ebb current velocities. Tidal asymmetry occurred mainly during the dry season and was not obvious in the wet season (Fig. 5b and e). The significant wave heights in the dry season were approximately 0.11 m on average (Fig. 5c), which were much higher than the ones in the wet season (only 0.04 m on average (Fig. 5f)). The low water depth during the wet season can be considered as one of the main reasons for the small wave heights due to the wave energy dissipation. In addition, the significant wave heights in the wet season were not high in the estuary; hence, the significant wave heights in the mud-flat were not high.

The relationship between the current velocities and significant wave heights was complicated. In the dry season, on the two first tidal days (10:30 AM 6th Feb. 2012–10:00 AM 8th Feb. 2012), the significant wave heights were not high (approximately 0.07 m on average – Fig. 5c) whereas on the other tidal days (10:30 AM 8th Feb. 2012–7:00 AM 12th Feb. 2012), the significant wave heights were higher (approximately 0.15 m on average – Fig. 5c). Meanwhile, the current velocities were similar during the time measured (Fig. 5b). However, the peak of the wave and the peak of the current

velocity occurred at the same time (Fig. 5b and c). Within the wet season, on the fifth tidal day (09:00 PM 24th Jun. 2014–12:00 PM 25th Jun. 2014), the significant wave heights were weak (Fig. 5f) but the current velocities were strong (Fig. 5e). The current velocities were similar during the time measured and higher at the flood tide. This proves that the current velocities were affected strongly by the tides.

Fig. 5a and d shows that the SSCs in the dry and wet seasons were similar (approximately 0.11 kg m^{-3} on average), but the fluctuation of SSCs in the dry season was stronger than the one in the wet season. In particular, at 01:00 AM 10th Feb. 2012, the peak SSC in the dry season reached 0.59 kg m^{-3} , and the peak SSC coincided with the maximum current velocity and high significant wave height (Fig. 5a). However, the anomalous value was quite different from the surrounding values.

In the dry season, the significant wave heights can reach up to 0.36 m (Fig. 5c). Under strong waves, from 8th Feb. 2012 to 12th Feb. 2012, the average SSC was 0.13 kg m^{-3} , while under weak waves, from 6th Feb. 2012 to 7th Feb. 2012, the average SSC was 0.06 kg m^{-3} (Fig. 5a and c). It can be shown that the SSCs during the high waves are more than twice as high as the SSCs during the small waves, which is similar to the results in the wet season. It can be explained

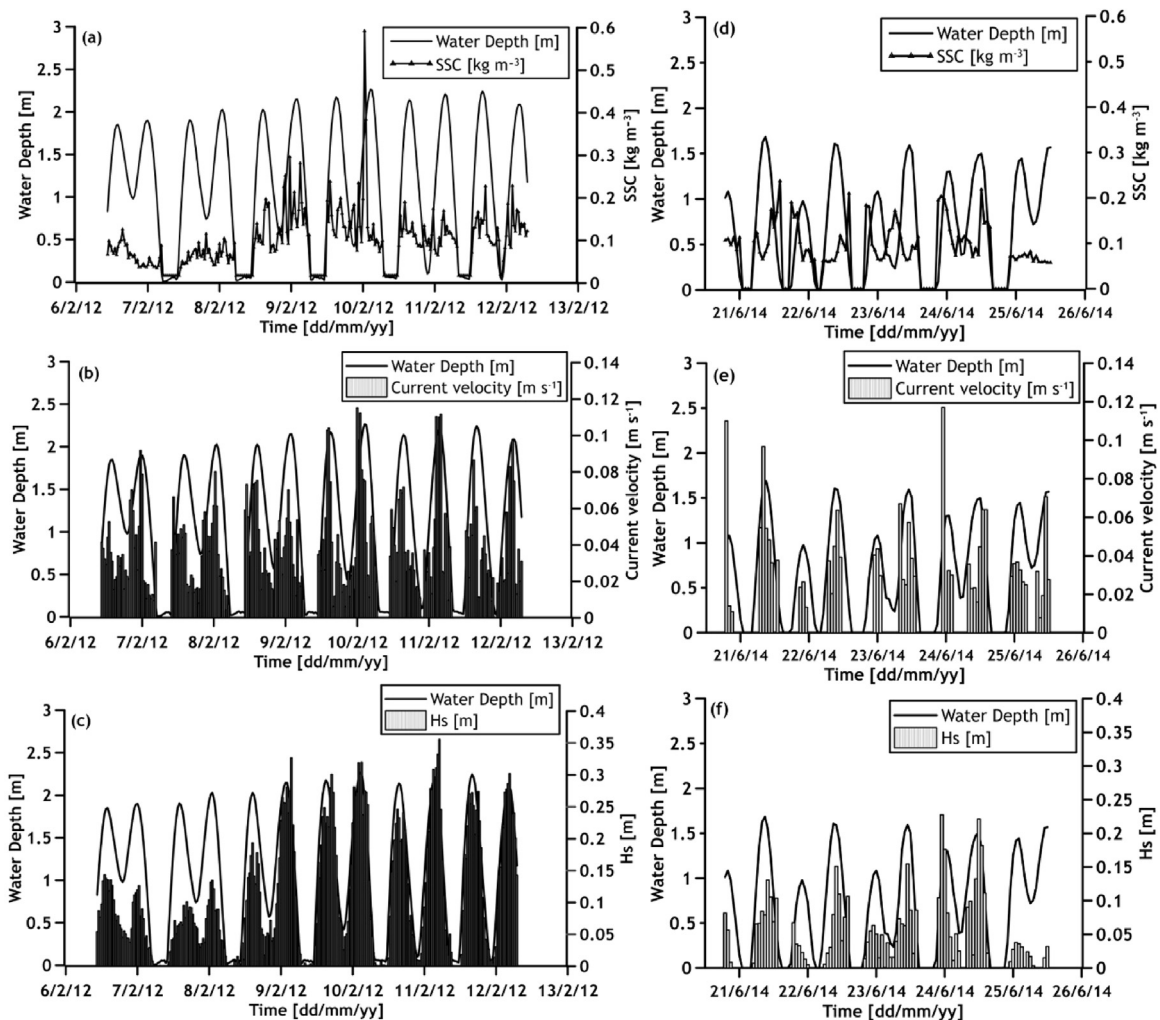


Figure 5 Water depths, SSCs, current velocities, and significant wave heights (Hs) in the mud flat (ST1) in the dry season (a–c) and the wet season (d–f).

that the high waves can pump up the suspended matters from the bottom and cause a higher turbulence.

The amount of SSC input or output to the mud-flat during the tidal cycles are different in both the dry and wet seasons. The deposition trend will occur when the SSCs during the flood tide are higher than during the ebb tide. In the opposite case, an erosion trend will occur. Fig. 5a shows that, in the dry season, the deposition trend was higher than the erosion trend. However, the deposition and erosion trends in the wet season were not clear (Fig. 5d). This may be due to the hydrodynamics of the waves and currents in the dry season being stronger than the ones in the wet season. In general, the deposition trend could be considered to be the main trend in the mud-flat for both seasons. The current velocity could be the main factor controlling the SSC distribution.

3.3. In the mangrove forest

Fig. 6 shows the bathymetry from the mud-flat to the mangrove forest on 25th Jun. 2014. There was a large difference (approximately 1.2 m) between the mud-flat station ST1 and the mangrove forest station ST2, hence the water levels in the

mangrove forest (ST2) were found to be low. The highest water level reached approximately 0.93 m in the dry season (Fig. 7a) and only 0.27 m in the wet season (Fig. 7d). Because the water level depths in the wet season were too low, the significant wave heights and the current velocities were small; hence, the impact of the hydrodynamics on SSCs could not be shown effectively (Fig. 7d–f). Therefore, only the hydrodynamics in the dry season can be considered in this section.

In the dry season, the significant wave heights and current velocities were also low. The maximum current velocity was found to be approximately 0.07 m s^{-1} (Fig. 7b) and the maximum significant wave height was approximately 0.36 m (Fig. 7c). The peak current velocities almost occurred at high slack water.

In the mangrove forest, the current velocities during the flood tide were higher than the ones during the ebb tide (Fig. 7b). Consequently, the average SSCs during the flood tide were higher than during the ebb tide (Fig. 7a). The SSCs changed in accordance with the current velocities. It proves that the current velocity played a more dominant role on the SSCs within the mangroves (ST2), especially when the water levels were low enough.

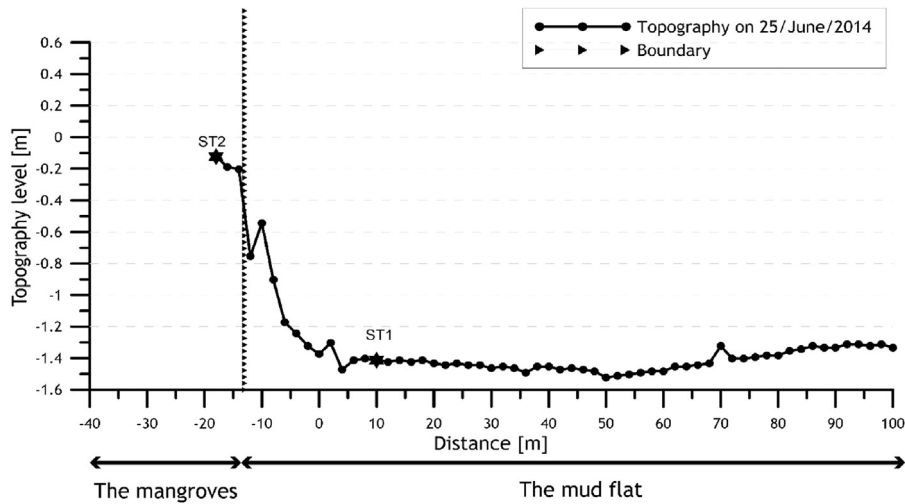


Figure 6 Topography at study site on 25th Jun. 2014.

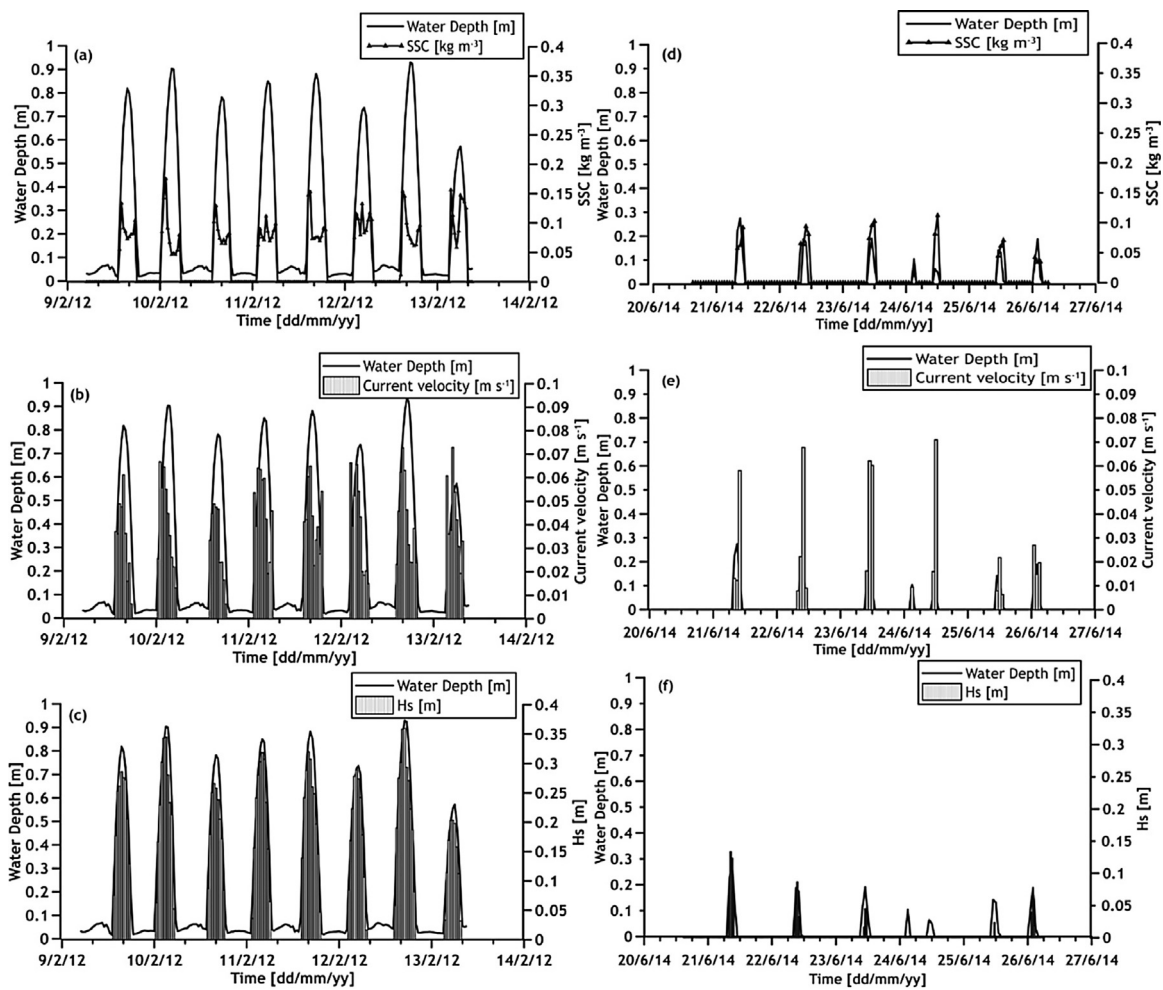


Figure 7 Water depths, SSCs, current velocities, and significant wave heights (Hs) in the mangroves (ST2) in the dry season (a–c) and the wet season (d–f).

Table 3 Calculated suspended sediment rate Q during the flood tides, ebb tides and total Q on one tidal day.

Cases	Station ST2 – in the mangrove forest		
	Q_{flood}	Q_{ebb}	Q_{tol}
Q [$\text{kg m}^{-1} \text{s}^{-1}$]			
<i>Case I: strong waves</i> (H_s average = 0.24 m)	$+22 \times 10^{-3}$	-6×10^{-3}	$+16 \times 10^{-3}$
<i>Case II: weak waves</i> (H_s average = 0.14 m)	$+12 \times 10^{-3}$	-4×10^{-3}	$+8 \times 10^{-3}$

Note: “+”: the seaward of Q , “-”: the landward of Q .

To illustrate the role of the mangrove forest in the accumulation during the dry season, the sediment transport rate Q (the suspended sediment transport per unit width) during the incoming tides and outgoing tides in one tidal period was calculated in Eq. (1) (Mehta and Li, 2003).

$$Q = \int_0^h U_{tol}(z)C(z)dz, \tag{1}$$

in which $C(z)$ is the vertical variation of the SSCs. $U_{tol}(z)$ is the total velocities in the water column due to the tidal currents and wave-induced velocity in Eq. (2).

$$U_{tol} = U_{tide} + U_{wave}. \tag{2}$$

It is found that the tidal currents are positive on the flood tide and negative on the ebb tide. Therefore, the value of the vertical sediment transport rate Q at the observed point will be positive for the tidal flow to the forest and negative for the tidal ebb to the ocean.

For practical applications, $U_{tol}(z)$ could be used as the mean total velocity due to the tides and waves. Because the water level depths in the mangrove were so low, the tidal currents and wave-induced velocities could be considered

vertically uniform. $U_{tol}(z)$ and $C(z)$ were based on the field experimental data at ST2.

The suspended sediment rate on one tidal day was calculated in two cases: strong waves (from 2:30 PM to 7:30 PM 12th Feb. 2012) and weak waves (from 3:30 AM to 7:30 AM 13th Feb. 2012). The calculated results at the study site are shown in Table 3.

For both cases of strong and weak waves, the suspended sediment rates at the flood tide were three times higher as the ones at the ebb tide. Therefore, the total suspended sediment rate Q_{tol} resulted in positive values. The total Q_{tol} under the strong waves was more than twice as high as the total Q_{tol} under the weak waves. This result indicates that the strong hydrodynamics caused high turbulence; therefore, the vertical suspended sediment rate Q_{tol} achieved high values as well. In addition, for the tidal flow to the mangrove forests, the vertical suspended sediment rate Q_{tol} had positive values.

In general, the mangrove SSCs were mainly affected by the currents. In addition, the SSCs during the flood tides were higher during the ebb tides. This proves the role of the mangrove forests in accumulation in the coastal area.

3.4. Topography and shoreline change

Fig. 8 shows how the topography at Nang Hai changed over three years (from 20th Jan. 2014 to 25th May 2017). The boundary between the mud-flat and the mangrove forest was being eroded rapidly. In one year (from Jan. 2014 to Feb. 2015), the mangrove boundary was shifted approximately 5 m inwards. In three years (from Jan. 2014 to May 2017), the boundary was shifted inwards approximately 25 m. Hence, the displacement rate was calculated at approximately $0.61 \text{ m month}^{-1}$ in 41 months (Jan. 2014–May 2017). Although the boundary between the mangrove and mud-flat had been eroded, the bathymetry in the mud-flat had accumulated during the measured time. In general, the range of the average depth deposition reached up to 0.40 m, but the

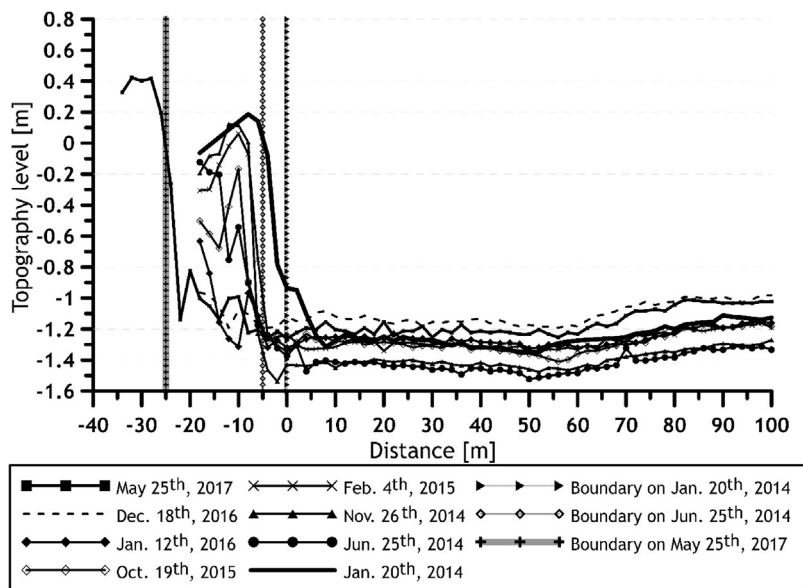


Figure 8 Changes in the topography at the study site from 2014 to 2017.

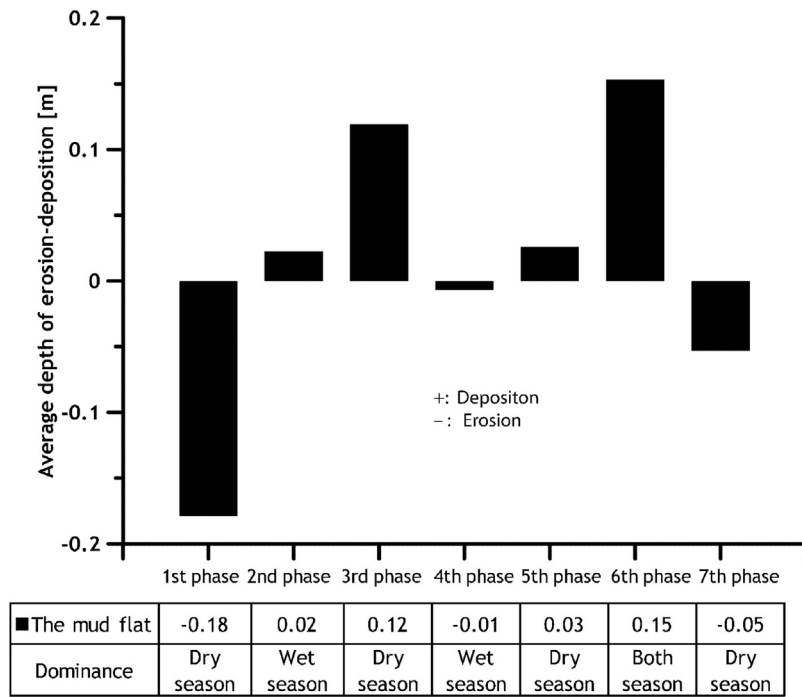


Figure 9 The erosion–deposition process from 2014 to 2017 in the mud flats (ST1).

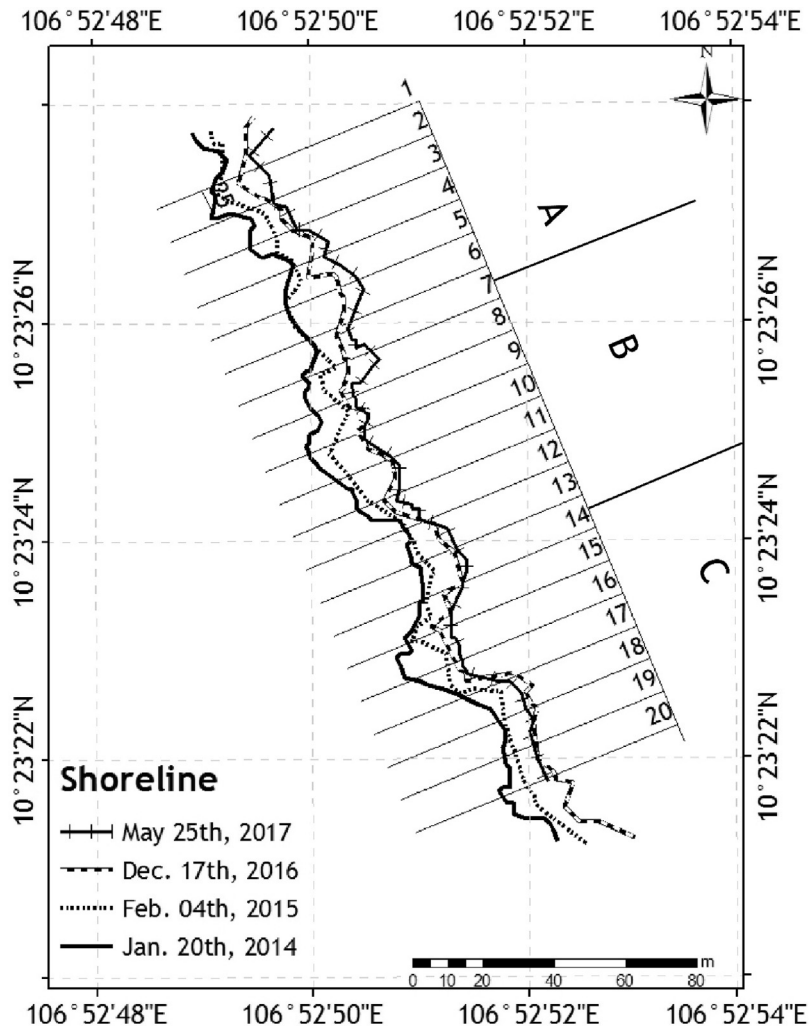


Figure 10 Measured shoreline changes from 2014 to 2017.

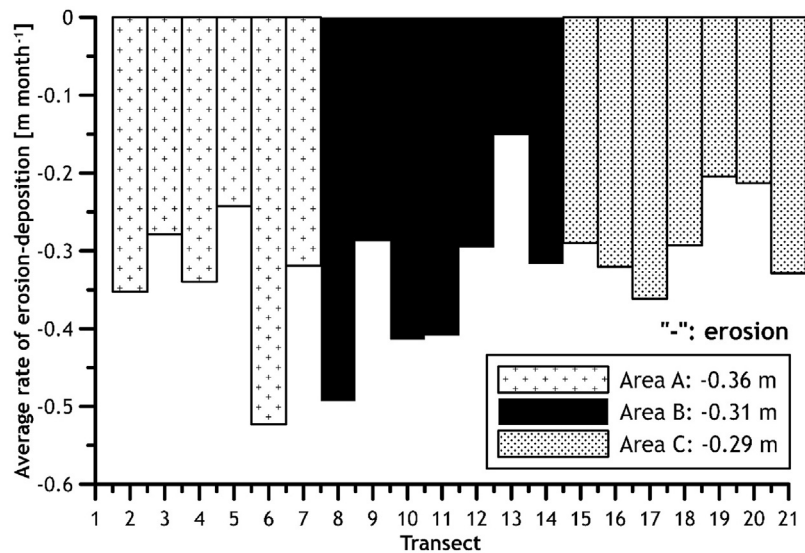


Figure 11 The average rate of erosion at the study site from 2014 to 2017.

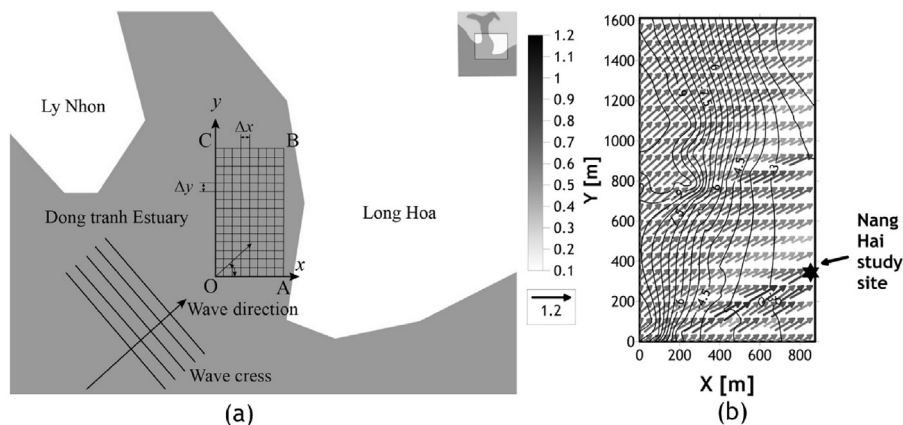


Figure 12 Calculated results at the Dong Tranh Estuary (Vo Luong et al., 2008): (a) the calculated area and (b) the result of the wave fields.

deposition and erosion processes occurred alternately. The measured SSC results at ST1 (Section 3.2) also proved that deposition occurred within the mud-flat. In the 1st, 3rd and 7th phases, the erosion process occurred, while the deposition process occurred in the 2nd, 4th, 5th and 6th phases. The deposition in the mud-flat could be explained by two reasons. First, the flood tides were strong enough to bring sediment into the mud-flat (Section 3.2). Second, the erosion at the boundary may contribute to the settlement of the sediment in the mud-flat. Fig. 9 shows that the difference in the sediment in the dry season was higher than that in the wet season. In the dry season, the average depth erosion reached up to 0.18 m in the first phase and to an average depth deposition of 0.12 m in the third phase. Meanwhile, in the wet season, the average depth erosion was 0.01 m in the 4th phase, while the average depth deposition was only 0.02 m in the 2nd phase.

Fig. 10 shows the observation of the mangrove shoreline changes by using GPS from 20th Jan. 2014 to 25th May 2017. In general, the entire shoreline used as the study site has been eroded. The shoreline was divided into three areas

(A, B and C), and the Nang Hai site was situated in area A where the strongest erosion process occurred. The degradation rate was calculated as approximately $0.36 \text{ m month}^{-1}$ in area A (Fig. 11). The results could be shown to be aligned with the results from the topography methods by using levelling instruments. However, the calculated rate of the cross-shore changes by topography was higher ($0.61 \text{ m month}^{-1}$). There were many possible causes, such as error from GPS instrument; error within the measurement recorded, or error from the calculation in ArcGIS (DSAS tool), etc. Moreover, by using the wave refraction model, Vo Luong et al. (2008) proved that the Nang Hai study site was affected strongly by the wave fields (Fig. 12). In summary, the higher the wave heights were, the stronger the erosion–deposition processes.

However, the causes of erosion at the study site were not only due to the hydrodynamics but also due to human activities. Previous studies, such as Mazda et al. (2002) and Vinh and Truong (2012), showed that human intervention also affected the erosion mechanism in the Nga Bay River, which is not far from the study site. In recent years, Tin and Vinh (2013) showed that sand extraction between the Dong Tranh

Gulf and Gan Ray Gulf affected the erosion–deposition processes significantly. These activities may impact the sediment mechanism, causing the erosion–deposition processes at the study site.

4. Conclusions

The observations and measurements from the mangrove areas of the Dong Tranh Estuary, Vietnam, showed strong relationships between the hydrodynamic processes and suspended sediment dynamics. In the estuary, the SSCs were very complicated due to the mixed impacts of the waves and currents in both seasons. The waves had a strong impact on the variability of the SSCs in the dry season. In the mud-flat, the current velocities were the main factor that dictated SSC distribution. In the mangrove forest, the SSCs were influenced strongly by the currents in the dry season and had a strong tidal asymmetry. Additionally, most of the measured results showed that the hydrodynamics in the dry season were stronger than the ones in the wet season. Hence, the hydrodynamics in the mangrove areas were influenced strongly by monsoons.

The results of the shoreline and topography changes show that in the mud-flat, the erosion and deposition processes occurred alternately, and that the deposition was more dominant than the erosion. The erosion–deposition intensity in the dry monsoon was stronger than the one in the wet monsoon. In the mangrove forest, the erosion process always occurred, especially at the sloping mangrove edge, where the erosion was at its strongest. The measured results showed that the hydrodynamics in the mangroves were weak; meanwhile, the hydrodynamics in front of the mangrove edge were strong. Thus, the hydrodynamics can be considered one of the causes of erosion in the mangrove edge.

In conclusion, similar to previous studies, this study is concurrent with a soil retention role for mangrove forests. However, the study site is being eroded. It is noticeable that the wave energy dissipation in the mangrove was not large, and that the wave energy dissipation occurred in the mud-flat due to the bottom topography. Human activity was not considered in the study. Additionally, the measured time in the study was not long enough and only occurred in the El Nino period (Nov. 2014–Apr. 2016). Hence, it is necessary to conduct future work for a longer term to determine the factors affecting the erosion–deposition processes at the study site.

Acknowledgements

This work was supported by the NAFOSTED (grant numbers: ĐT. NCCB-ĐHU'D.2012-G/10). We would like to express our great gratitude to late Professor Stanislaw Massel for the invaluable advice.

References

- Bao, T.Q., 2011. Effect of mangrove forest structures on wave attenuation in coastal Vietnam. *Oceanologia* 53 (3), 807–818, <http://dx.doi.org/10.5697/oc.53-3.807>.
- Bay, N.T., Toan, T.T., Phung, N.K., Tri, N.Q., 2012. Numerical investigation on the sediment transport trend of can Gio Coastal Area (Southern Vietnam). *J. Mar. Environ. Eng.* 9 (3), 191–210.
- Bryce, S., Larcombe, P., Ridd, P.V., 2003. Hydrodynamic and geomorphological controls on suspended sediment transport in mangrove creek systems, a case of study: Cocoa Creek, Townsville, Australia. *Estuar. Coast. Shelf Sci.* 56 (3–4), 415–531, [http://dx.doi.org/10.1016/S0272-7714\(02\)00192-0](http://dx.doi.org/10.1016/S0272-7714(02)00192-0).
- Cao, H., Chen, Y., Tian, Y., Feng, W., 2016. Field investigation into wave attenuation in the mangrove environment of the South China Sea Coast. *J. Coastal Res.* 32 (6), 1417–1427, <http://dx.doi.org/10.2112/JCOASTRES-D-15-00124.1>.
- Capo, S., Sottolichio, A., Brenon, I., Castaing, P., Ferry, L., 2006. Morphology, hydrography and sediment dynamics in a mangrove estuary: the Konkoure Estuary, Guinea. *Mar. Geol.* 230 (3–4), 199–215, <http://dx.doi.org/10.1016/j.margeo.2006.05.003>.
- FAO, 2015. *Global Forest Resources Assessment 2015. Food and Agriculture Organization of the United Nations*, 244 pp.
- Furukawa, K., Wolanski, E., 1996. Sedimentation in mangrove forest. *Mang. Salt Marsh.* 1 (1), 3–10.
- Hong, P.N., San, H.T., 1993. *Mangroves of Vietnam. IUCN—The World Conservation Union, Bangkok, Thailand*, 173 pp.
- Horstman, E.M., Dohmen-Janssen, C.M., Narra, P.M.F., van den Berg, N.J.F., Siemerink, M., Hulscher, S.J.M.H., 2014. Wave attenuation in mangroves: a quantitative approach to field observations. *Coast. Eng.* 94, 47–62, <http://dx.doi.org/10.1016/j.coastaleng.2014.08.005>.
- Li, L., Wang, X.H., Andutta, F., Williams, D., 2014. Effects of mangroves and tidal flats on suspended-sediment dynamics: Observation and numerical study of Darwin Harbour, Australia. *J. Geophys. Res.-Oceans* 119 (9), 5854–5873, <http://dx.doi.org/10.1002/2014JC009987>.
- Massel, S.R., Furukawa, K., Brinkman, R.M., 1999. Surface wave propagation in mangrove forests. *Fluid Dyn. Res.* 24 (4), 219–249, [http://dx.doi.org/10.1016/S0169-5983\(98\)00024-0](http://dx.doi.org/10.1016/S0169-5983(98)00024-0).
- Mazda, Y., Magi, M., Kogo, M., Hong, P.N., 1997. Mangroves as a coastal protection from waves in the Tong King Delta, Vietnam. *Mang. Salt Marsh.* 1 (2), 127–135.
- Mazda, Y., Magi, M., Nanao, H., Kogo, M., Miyagi, T., Kanazawa, N., Kobashi, D., 2002. Coastal erosion due to long-term human impact on mangrove forests. *Wetl. Ecol. Manag.* 10 (1), 1–9, <http://dx.doi.org/10.1023/A:1014343017416>.
- Mazda, Y., Magi, M., Ikeda, Y., Kurokawa, T., Asano, T., 2006. Wave reduction in a mangrove forest dominated by *Sonneratia* sp. *Wetl. Ecol. Manag.* 14 (4), 365–378, <http://dx.doi.org/10.1007/s11273-005-5388-0>.
- Mehta, A., Li, Y., 2003. *Principles and Process – Modelling of Cohesive Sediment Transport. University of Florida*, 86 pp.
- Norris, B.K., Mullarney, J.C., Bryan, K.R., Henderson, S.M., 2017. The effect of pneumatophore density on turbulence: a field study in a *Sonneratia*-dominated mangrove forest, Vietnam. *Cont. Shelf Res.* 147, 114–127, <http://dx.doi.org/10.1016/j.csr.2017.06.002>.
- Parvathy, K.G., Bhaskaran, P.K., 2017. Attenuation in presence of mangrove: a sensitivity study for varying bottom slopes. *Int. J. Ocean Climate Syst.* 8 (3), 126–134, <http://dx.doi.org/10.1177/1759313117702919>.
- Phuoc, V.L.H., 2012. *Concentration of suspended sediments in mangrove forests (Nang Hai study site, Ho Chi Minh city). Scientific research project of Viet Nam National University – Ho Chi Minh city (in Vietnamese)*.
- Saenger, P., 2002. *Mangrove Ecology, Silviculture and Conservation. Kluwer Academic Publishers, Netherlands*, 360 pp.
- Schwarzer, K., Thanh, N.C., Ricklefs, K., 2016. Sediment re-deposition in the mangrove environment of Can Gio, Sai Gon River estuary (Vietnam). *J. Coastal Res.* 75 (Sp. Iss.), 138–142, <http://dx.doi.org/10.2112/SI75-028.1>.
- Shepard, C.C., Crain, C.M., Beck, M.W., 2011. The protective role of coastal marshes: a systematic review and Meta-analysis. *PLoS ONE* 6 (11), e27374, <http://dx.doi.org/10.1371/journal.pone.0027374>.

- Tin, H.T., Vinh, B.T., 2013. Exploitation, evaluation of reserve and environmental impact assessment of the sand extraction in Can Gio coastal zone. Kick-off Seminar on ASEAN-Japan Build-up Cooperative Education Program for Global Human Resource Development in Earth Resources Engineering. Bangkok, Thailand.
- Van Santen, P., Augustinus, P.G.E.F., Janssen-Stelder, B.M., Quartel, S., Tri, N.H., 2007. Sedimentation in an estuarine mangrove system. *J. Asian Earth Sci.* 29 (4), 566–575, <http://dx.doi.org/10.1016/j.jseaes.2006.05.011>.
- Vinh, B.T., Truong, N.H., 2012. Erosion mechanism of Nga Bay Riverbanks (Ho Chi Minh City, Vietnam). *ASEAN Eng. J. C* 3 (2), 132–141.
- Vo Luong, H.P., Toan, N.D., An, D.T., Hanh, T.C., 2008. Computation of wave field in the Dong Tranh estuary, can Gio by using wave refraction model. *J. Geol. Ser. B* 31–32, 164–170.
- Vo Quoc, T., Kuenzer, C., 2012. Can Gio Mangrove Biosphere Reserve Evaluation 2012: Current Status, Dynamics and Ecosystem Services. IUCN, Ha Noi, Vietnam, 100 pp.
- Vo-Luong, H.P., Massel, S.R., 2006. Experiment on wave motion and suspended sediment concentration at Nang Hai, Can Gio mangrove forest, Southern Viet Nam. *Oceanologia* 48 (1), 23–40.
- Vo-Luong, H.P., Massel, S.R., 2008. Energy dissipation in non-uniform mangrove forests of arbitrary depth. *J. Mar. Syst.* 74 (1–2), 603–622, <http://dx.doi.org/10.1016/j.jmarsys.2008.05.004>.
- Wolanski, E., 1995. Transport of Sediment in mangrove swamps. *Hydrobiologia* 295 (1–3), 31–42.